

# Interactive determination of robust safety margins for oncologic liver surgery

Christian Hansen · Stephan Zidowitz ·  
Milo Hindennach · Andrea Schenk ·  
Horst Hahn · Heinz-Otto Peitgen

Received: 12 January 2009 / Accepted: 5 May 2009  
© CARS 2009

## Abstract

**Objective** Complex oncologic interventions in the liver require an extensive and careful preoperative analysis. Particularly the achievement of an optimal safety margin around tumors remains a difficult task for surgeons.

**Methods** We present new methods for evaluating different safety margins and their effect on the associated interruption of vascular supply or drainage. The characteristic of vascular risk distributions can be evaluated in real-time by exploiting precomputed safety maps that provide a volume curve for each vascular system. By applying fast visualization methods in 3D it is possible to assist the surgeon in the determination of a tumor-free safety margin while preserving sufficient vital hepatic parenchyma. The combination of risk analysis from different vascular systems and their sensitivity is considered.

**Results** We provide physicians with a novel computer-aided planning tool that allows for interactive determination of safety margins in real-time. The planning tool integrates smoothly into the preoperative workflow. Preliminary evaluations confirm that the width of safety margins can be determined more precisely, which may affect the proposed resection strategy.

**Conclusion** Our new methods provide interactive feedback and support for decision making during the preoperative planning stage and thus might potentially improve the outcome of surgical interventions.

**Keywords** Liver surgery planning · Oncologic risk analysis · Real-time interaction · Visualization

## Introduction

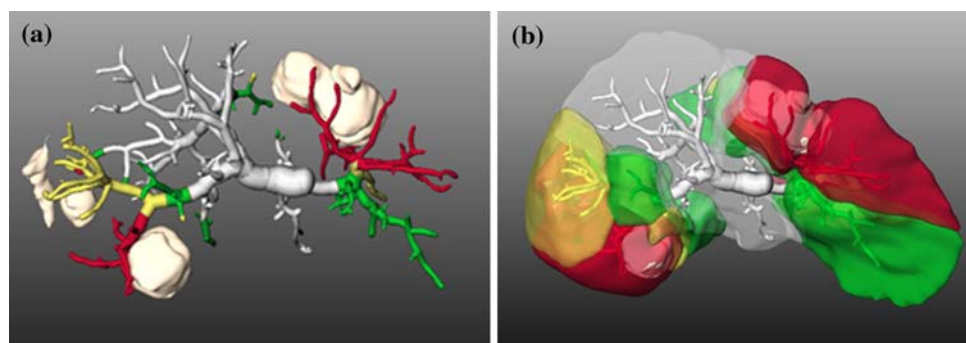
A main factor for a good patient outcome in oncologic liver surgery is the complete excision of all tumors, including a tumor-free safety margin (R0-resection). A positive safety margin (R1-resection) is considered a very poor prognostic factor, comparable to the presence of satellite metastases [1]. However, when removing a tumor and its safety margin, adjacent vessels have to be transected. These vessels supply or drain a dedicated liver region and thus define a territory at risk. Therefore, the number of vessels that can be preserved correlates with the postoperative residual liver volume, which has to be at least 20% of the total estimated liver volume for normal parenchyma; 30–60% if the liver is injured by chemotherapy, steatosis, or hepatitis; or even 40–70% in the presence of cirrhosis [2]. Taking into account that the liver contains four different vascular systems (portal vein, hepatic vein, hepatic artery, bile duct), the assessment of combined territories at risk is not trivial.

The determination of optimal safety margins around tumors in the liver is a challenging task for a surgeon. Size, number and location of tumors and their relation to the intra-hepatic vascular anatomy, are all important factors in deciding whether a tumor-free safety margin can be achieved while preserving sufficient vital hepatic parenchyma [1]. From the medical point of view, a wider safety margin theoretically gives a higher potential for cure, while a smaller safety margin (e.g. <1 cm for colorectal metastases) should not be an exclusion criterion for resection [3]. However, the width of the margin may impair in- and out-flow of the blood in the liver, which increases the incidence of postoperative liver failure. In particular, primary liver cancer where a residual volume of at least 40% is required, is often inoperable due to the extent of liver cirrhosis accompanying the cancer.

---

C. Hansen (✉) · S. Zidowitz · M. Hindennach · A. Schenk ·  
H. Hahn · H.-O. Peitgen  
Fraunhofer MEVIS, Institute for Medical Image Computing,  
Bremen, Germany  
e-mail: Christian.Hansen@mevis.fraunhofer.de

**Fig. 1** Risk analysis for the portal vein with adjacent metastases. **a** The visualization of vessels at risk simulates affected branches when using a safety margin of 5 mm (*red*), 10 mm (*yellow*) or 15 mm (*green*). **b** Based on the analysis of vessels at risk dedicated territories at risk are computed



From the mathematical point of view, it is important to know that the location and extent of territories at risk are sensitive to small changes in the width of the safety margin. However, there exist safety margins with a “robust” risk where changes to the width of the margin alter the territories at risk only to a limited extent. Our aim is to provide physicians with a computer-aided planning tool with which different risk margins can be evaluated in adequate time.

## Methods

In this section we briefly review prior work concerning oncologic risk analyses for liver surgery planning. Subsequently, we present new methods for the determination of robust safety margins as well as the combination of oncologic risk analyses.

### From voxels to risk analyses

The reconstruction of 3D planning models and associated risk analyses are an integral part of the software assistant *MeVisLiverAnalyzer* [4], which comprises all steps for analyzing contrast-enhanced CT and MRI data for preoperative planning in liver surgery. We briefly describe the important steps for vascular analysis and visualization as introduced in [5]: vascular structures are segmented semi-automatically using a threshold-based region-growing technique. Skeletonization with a topology-preserving thinning algorithm yields an exact centerline and vessel radii at each voxel of the skeleton. A graph analysis transforms the vessel skeleton in a directed, acyclic graph where nodes represent furcations. Based on the assumption of a circular cross-section of vasculature, smooth transitions at furcations and rounded ends are produced by means of truncated cones to provide an abstract visualization. Tumors and liver surface are segmented semi-automatically [6,7] and transformed to a triangle mesh.

For the visualization of affected vessels, the spatial relations between tumors and vessels have to be analyzed. Preim

et al. [8] proposed a method which assumes a limited number of virtual safety margins around tumors. The standard widths were set to 5, 10 and 15 mm. By default, red color is employed for the 5 mm margin, which is assumed to be resected; yellow and green for larger margins. For determination of the vascular branches within a certain safety margin around the tumor, the border voxels are detected by calculating the difference of the tumor and an eroded mask, using a  $3 \times 3 \times 3$  structuring element for erosion. Distance transformation is applied to all border voxels, affected vessels are identified and relabeled depending on the predefined safety margins (Fig. 1a). Furthermore, a Voronoi tessellation of the liver volume according to the centerline voxels of the segmented vascular structure approximates the volume of the parenchyma supplied or drained by the affected vessels. For each safety margin the territories at risk are quantitatively analyzed. Finally, an iso-surface renderer generates separate triangle meshes and sets vertex colors (Fig. 1b).

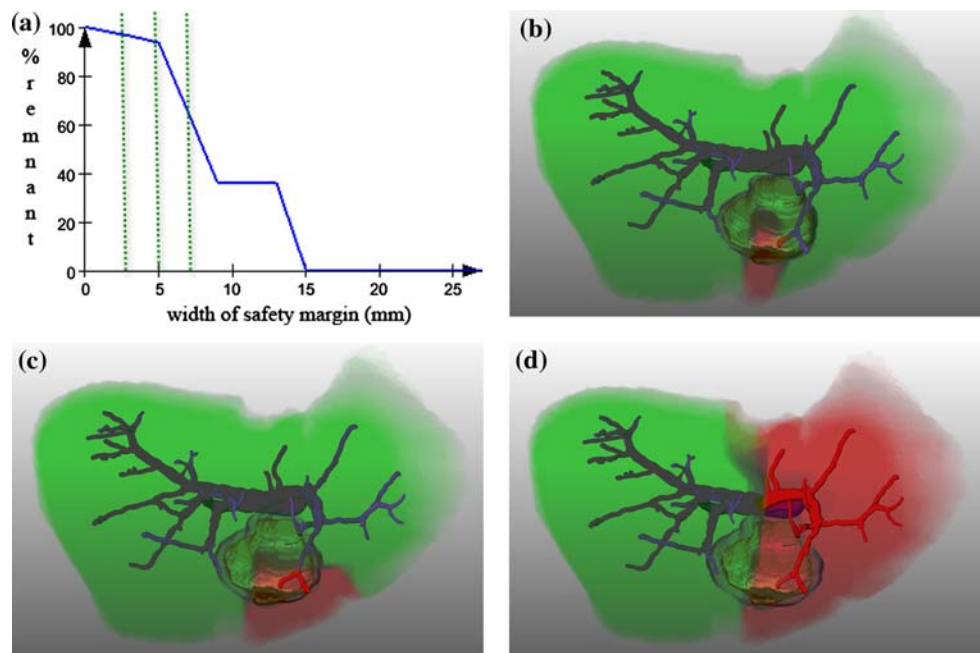
### Determination of robust safety margins using a vascular system

Standard widths for safety margins as proposed in [8] can be computed automatically in order to assess surgical difficulty, but they do not allow for detailed exploration of surgical feasibility. There exist two computational bottlenecks in the pipeline described above that make an interactive exploration of arbitrary safety margins impossible:

- (1) computation of territories at risk for specific safety margins in image space, and,
- (2) update of the 3D visualization.

The computation time for these steps is approximately 10 s on a standard workstation. In order to accelerate the first process (1), we introduce a so-called “safety map” for each vessel system which is calculated in a preprocessing step. The safety map encodes the margin at which each voxel of the liver parenchyma will be affected by the tumor. Following a nearest neighbor distance model, a Voronoi tessellation

**Fig. 2** Volume curve for a portal vein (a) with dedicated 3D visualization for safety margins of 3 mm (b), 5 mm (c), and 7 mm (d). A margin >5 mm is associated with a high sensitivity of risk



of the liver volume according to the centerline voxels of the segmented vascular structure approximates the perfusion or drainage areas. Combining this information with a distance transformation with respect to the tumor boundary, and taking the hierarchical dependencies of the vascular tree into account, the safety map for a specific vascular tree of the liver can be calculated. The map can be used as a 3D look-up table, where the query of affected voxels (territories at risk) for a specific safety margin can be found in linear computation time.

The quantification of territories at risk as a function of the safety margin is extracted from these maps by histogram analysis. To highlight safety margins that are sensitive to small changes, we provide the user with a risk graph that contains cumulative histograms (volume curves) for each vessel system (Fig. 2a). A vertical slider in the risk graph is used to modify the width of a specific safety margin. The discontinuities in the compromised volume curves correspond to the transection of major vessels, setting the dependent territories at risk. Hence, these curve-discontinuities directly correspond to sensitive parameters for the surgical planning. Given that the corresponding safety margin is required to guarantee the R0-resection, the surgeon has to decide whether the loss of functional volume in this magnitude can be tolerated.

The spatial visualization of territories at risk and affected vessels with respect to the current safety margins is important to evaluate the surgical feasibility. To update the 3D visualization of territories at risk (2) upon modifications of the safety margin, we use a fast direct volume rendering technique that applies a transfer function on the precomputed safety map. The volume rendering is mixed with the model-based representation of vascular trees (Fig. 2b–d), while affected ves-

sels are labeled in red to highlight the relation between territories at risk and the supplying or draining vessels at risk. Quantitative information, mainly the affected liver volume (number of affected voxels) enhances the visualization. Compared to previous approaches, the visualization of territories at risk can be adapted in real-time which allows for a fast and detailed exploration of individual anatomic datasets.

To assess the validity of territories at risk, it is essential that the result can also be displayed in a 2D slice view. For this purpose, the simulation of territories at risk is superimposed with the original radiologic data. Furthermore, the user can generate iso-surfaces of the territories at risk for arbitrary margins to allow platform-independent utilization, e.g. in the operating room.

#### Combination of oncologic risk analyses

A combination of risk analyses from two or more vascular systems obtains acceptance in clinical routine [9, 10]. The importance of the venous drainage has been underestimated in the past. A venous congestion can result in restricted outflow, stasis of the blood in the arterial or portal venous system, and thrombosis. Thus, the combination of risk analyses and a fast determination of an optimal safety margin (considering each vascular system) is important to optimize a preoperative resection plan.

While the combination of vessels at risk requires a simultaneous visualization of all risk-labeled vessel systems (Fig. 3a), the combination of territories at risk is even more complex, since the risk territories of each vessel system overlap one another.

**Fig. 3** Combination of vessels at risk: **a** tumors are visualized in *yellow* with a *black*, semi-transparent safety margin, while affected branches are labeled in *red*, unaffected branches in *magenta* (portal vein) and *blue* (hepatic vein). **b** Risk graph containing volume curves of the hepatic vein (*red*), portal vein (*blue*), union (*solid black*) and intersection (*dashed black*)

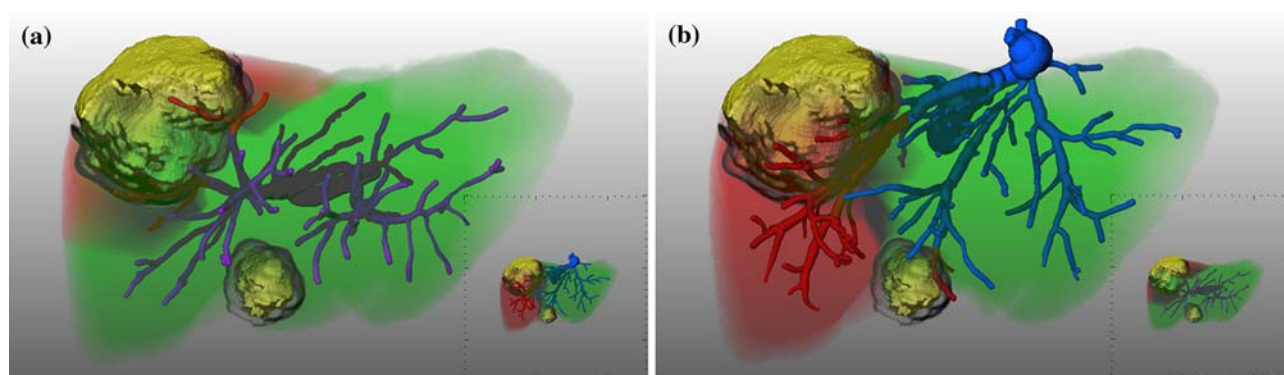
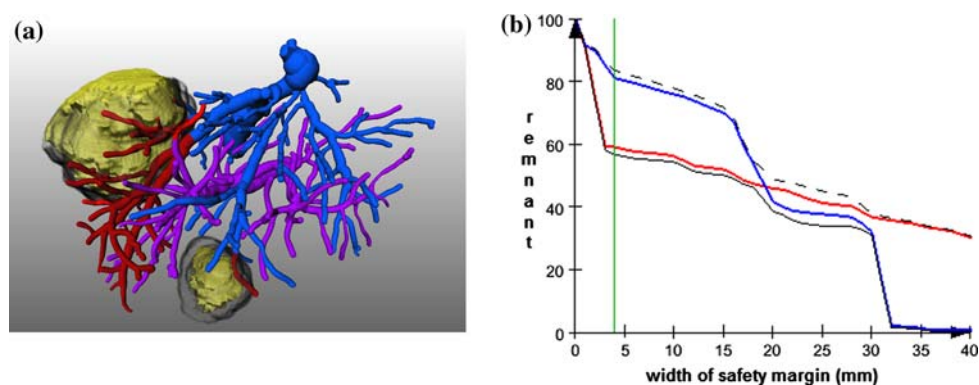


**Fig. 4** Combination of territories at risk using a picture-in-picture function. Affected parenchyma supplied by the portal vein is magnified while the interruption of vascular drainage (hepatic vein) is presented

as context information in (a), and vice versa in (b). The width of the security margin is set to 3.9 mm, and the underlying patient data are the same as in Fig. 3

For the exploration of combined risk we enhance the risk graph by volume curves of all segmented vascular systems (Fig. 3b). This allows for fast comparison of volume curves and their mutual sensitivity of risk. For the 3D visualization, we apply a picture-in-picture function with synchronized cameras for simultaneous visualization of different risk analyses in a single viewport. Thus, one vascular risk analysis can be focused by the user while providing information about further risk analyses as context information inside a specified viewport subregion (Fig. 4).

Based on the risk analysis for a given safety margin that is defined by the surgeon or derived from the safety map function, we can compute the risk territories for all segmented vascular structures. The union of territories at risk from different vascular systems can then be computed by assigning each voxel the minimum value of the individual safety maps, while the maximum value is assigned when calculating the intersection volume. It is obvious that the intersection of these territories should be part of the resection volume as it includes the tumor and represents a region without supply and drainage. However, defining a virtual resection plane does not mean to use the borders of territories at risk for this purpose, since territories for the different vascular systems overlap

with each other. The removal of any of these territories will cut-off some primarily non-affected parts of the other vascular systems. Hence, the removal of a primary territory at risk from a vascular tree causes the so-called “cascading of risk”, which in general enlarges the affected volumes induced by the other vascular systems and vice versa.

In order to support the definition of a proper virtual resection plane [11, 12] that includes the tumor with the determined safety margin, a combined visualization of different territories at risk within a single liver model is valuable. Therefore, we classify the affected liver volume in segments of:

- (1) impaired outflow,
- (2) impaired inflow, and;
- (3) impaired in- and outflow.

Thus, spatial overlaps of territories at risk which result in a visual clutter are prevented. Furthermore, the resulting visualization allows for the accentuation of vessels that cause a cascading of risk. An optimal resection proposal would consider this information in order to preserve these vascular structures from damage (Fig. 5).

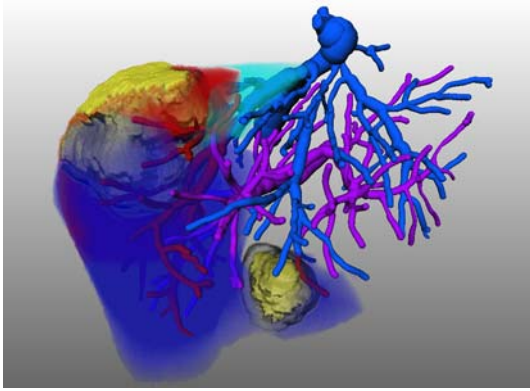


**Fig. 5** Combination of territories at risk by dividing the affected liver volume in segments of impaired outflow (*dark blue*), impaired inflow (*light blue*), and impaired in- and outflow (*red*). The width of the security margin and the underlying patient data are the same as in Figs. 3 and 4

## Results and conclusion

We provide a novel computer-aided planning tool for interactive determination of safety margins in real-time. Our new method shows additional information which is not directly visible in the radiologic data. It enhances approved methods for oncologic risk analysis [8] by allowing interactive feedback about the effect on the associated disruption of vascular supply or drainage. Furthermore, the resulting visualization of combined territories at risk can be used to optimize oncologic resection proposals.

The planning tool is available as an add-on for the planning software *MeVis LiverAnalyzer* [4] and integrates smoothly into a preoperative planning workflow. Preliminary evaluations confirm that the width of safety margins can be determined more precisely due to the interactive in-depth analysis, which may affect the proposed resection strategy. A quantitative user study with a large, representative selection of oncologic cases is currently in progress. To prove the clinical benefit of the new methods, a clinical evaluation is desirable. This requires a study with a randomized decision of whether or not to utilize the results of the risk analysis and the subsequent evaluation of clinical criteria, i.e. patient outcome in terms of 5-year-survival, complication rate, tumor recurrence, blood loss and others. There exists two reasons why this standard evaluation procedure is not suitable for the software-assisted risk analysis. First, it is ethically not justified to leave out information that helps the physician in decision making and operation planning; and second, the clinical criteria of the study depend on multiple factors, e.g. anamnesis of the patient, degree of liver steatosis, experience of the surgeon, or surgical technique that would require an enormous number of cases for reliable conclusions from the statistical point of view. Nevertheless, it is possible to analyze certain aspects for application of the oncologic risk analysis. Lang

et al. [9] showed for 15 oncologic resections, that the surgical strategy was changed in one-third of the cases when taking the results of the risk analysis into account. Other clinical partners have approved the usefulness of the risk analysis and preoperative planning for oncologic surgery [1, 10, 13, 14].

The proposed method assigns liver voxels to certain sections of the intrahepatic trees. From the anatomical point of view there exists a scaling problem, i.e. those sections of the vessels tree that actually drain a liver territory are usually not traceable in the image data because they are too small. The choice of a model-based approximation is difficult since the blood supply and drainage is realized by complex branching structures, whose formation process is not fully understood. We choose Voronoi tessellation with a nearest neighbor distance model to approximate these territories; studies on human corrosion casts revealed the accuracy of this approximation technique for the prediction of vascular territories [5]. Since the accuracy correlates significantly with the quality of the underlying volume data, reliable predication on liver tissue at risk have to consider the quality of the vessel segmentation (branching generation). Therefore, a proper visualization of data uncertainty would represent a valuable extension of the proposed risk analysis.

Furthermore, our method allows for the planning of safety margins considering sub-centimeter width. The question arises if this accuracy is necessary for preoperative planning since it can generally not be realized during common liver interventions. However, recent developments in navigated liver surgery show that a precise transfer of planning data in the operating room is feasible [15].

In our work, we have analyzed the risk distribution and the influence of the security margin width in detail. In order to provide a resection proposal, the desired resection plane has to be defined manually using a deformable cutting plane in 3D [11], and the visualization of combined territories at risk. But how can we calculate an adequate resection plane for a specific individual patient fully automatically? In many cases, an optimal resection plane is located between the intersection and the union of all territories at risk. In addition to the results of the risk analysis several other factors have to be considered for an adequate resection proposal such as the access to the tumor, a minimal resection surface, sufficient remnant volume, consideration of typical, well-experienced resection types (e.g. hemihepatectomy), and the option of alternatives such as radiofrequency ablation. Thus, the generation of automated resection proposals is part of future research.

**Acknowledgements** This work was funded by the German Federal Ministry of Education and Research (SOMIT-FUSION project FKZ 01—BE03C). The authors express gratitude to all involved physicians of the FUSION-project, in particular Karl Oldhafer, Gregor Stavrou (General Hospital Celle, Germany), and Hauke Lang (University Hospital Mainz, Germany) for fruitful discussions.

## References

1. van Ooijen PMA, Wolf R, Schenk A, Rouw DB, Slooff M, Peitgen HO, Oudkerk M (2003) Recent developments in organ-selective reconstruction and analysis of multiphase liver CT. *Imaging Decis MRI* 7(1):37–43. doi:[10.1046/j.1617-0830.2003.70105.x](https://doi.org/10.1046/j.1617-0830.2003.70105.x)
2. Pawlik TM, Schulick RD, Choti MA (2008) Expanding criteria for resectability of colorectal liver metastases. *Oncologist* 13(1): 51–64. doi:[10.1634/theoncologist.2007-0142](https://doi.org/10.1634/theoncologist.2007-0142)
3. Salloum C, Castaing D (2008) Surgical margin status in hepatectomy for liver tumors. *Bull Cancer* 95(12): 1183–1191
4. Schenk A, Zidowitz S, Bourquain H, Hindennach M, Hansen C, Hahn H, Peitgen HO (2008) Clinical relevance of model based computer-assisted diagnosis and therapy. *Proc SPIE Med Imaging* 6915(1):691502\_1–691502\_19
5. Selle D, Preim B, Schenk A, Peitgen HO (2002) Analysis of vasculature for liver surgical planning. *IEEE Trans Med Imaging* 21(11):1344–1357. doi:[10.1109/TMI.2002.801166](https://doi.org/10.1109/TMI.2002.801166)
6. Moltz JH, Bornemann L, Kuhnigk JM, Dicken V, Peitgen E, Meier S, Bolte H, Fabel M, Bauknecht HC, Hittinger M, Kiessling A, Püsken M, Peitgen HO (2009) Advanced segmentation techniques for lung nodules, liver metastases, and enlarged lymph nodes in CT Scans. *IEEE J Sel Top Signal Process* 3(1): 122–134. doi:[10.1109/JSTSP.2008.2011107](https://doi.org/10.1109/JSTSP.2008.2011107)
7. Schenk A, Prause G, Peitgen HO (2000) Efficient semiautomatic segmentation of 3D objects in medical images. In: *Proceedings of medical image computing and computer-assisted intervention (MICCAI)*, pp. 186–195
8. Preim B, Bourquain H, Selle D, Oldhafer KJ, Peitgen HO (2002) Resection proposals for oncologic liver surgery based on vascular territories. *Int J CARS* 1: 353–358
9. Lang H, Radtke A, Hindennach M, Schroeder T, Frühauf N, Malag M, Bourquain H, Peitgen HO, Oldhafer KJ, Broelsch CE (2005) Impact of virtual tumor resection and computer-assisted risk analysis on operation planning and intraoperative strategy in major hepatic resection. *Arch Surg* 140:629–638. doi:[10.1001/archsurg.140.7.629](https://doi.org/10.1001/archsurg.140.7.629)
10. Endo I, Shimada H, Takeda K, Fujii Y, Yoshida K, Morioka D, Sadatoshi S, Togo S, Bourquain H, Peitgen HO (2007) Successful duct-to-duct biliary reconstruction after right hemihepatectomy. Operative planning using virtual 3D reconstructed images. *J Gastrointest Surg* 11(5):666–670 doi:[10.1007/s11605-007-0130-2](https://doi.org/10.1007/s11605-007-0130-2)
11. Konrad-Verse O, Preim B, Littmann A (2004) Virtual resection with a deformable cutting plane. In: *Proc Simulation und Visualisierung*, pp 203–214
12. Pianka F, Schöbinger M, Müller S, Tetzlaff R, Büchler M, Gutt C, Weitz J, Schmidt J, Meinzer HP, Schmied B (2008) Clinical evaluation of a novel resection planning tool in hepatic surgery. *Suppl Int J Comput Assist Radiol Surg* 3(1): 381–382
13. Fuchs J, Warmann SW, Szavay P, Kirschner HJ, Schäfer JF, Hennemuth A, Scheel-Walter HG, Bourquain H, Peitgen HO (2005) Three-dimensional visualization and virtual simulation of resections in pediatric solid tumors. *J Pediatr Surg* 40(2):364–370. doi:[10.1016/j.jpedsurg.2004.10.026](https://doi.org/10.1016/j.jpedsurg.2004.10.026)
14. Endo I, Shimada H, Sugita M, Fujii Y, Morioka D, Takeda K, Sugae S, Tanaka K, Togo S, Bourquain H, Peitgen HO (2007) Role of three-dimensional imaging in operative planning for hilarcholeangioma. *Surgery* 142(5):666–675. doi:[10.1016/j.surg.2007.05.018](https://doi.org/10.1016/j.surg.2007.05.018)
15. Markert M, Nowatschin S, Weber S, Hansen C, Zidowitz S, Bourquain H, Stavrou GA, Oldhafer KJ, Peitgen HO, Lueth TC (2008) Navigated resection of residual liver tumors that are no longer visible after presurgical chemotherapy. *Suppl Int J Comput Assist Radiol Surg* 3(6):599–600. doi:[10.1007/s11548-008-0256-z](https://doi.org/10.1007/s11548-008-0256-z)